Anisotropic optical conductivity of $Sr_4Ru_3O_{10}$

C. Mirri,[1] F. M. Vitucci,[1] P. Di Pietro,[1] S. Lupi,[2] R. Fittipaldi,[3] V. Granata,[3] A. Vecchione,[3] U. Schade,[4] and P. Calvani[1]

[1]*CNR-SPIN and Dipartimento di Fisica, Università di Roma La Sapienza, Piazzale A. Moro, 2, I-00185 Roma, Italy*

[2]*CNR-IOM and Dipartimento di Fisica, Università di Roma La Sapienza, Piazzale A. Moro, 2, I-00185 Roma, Italy*

[3]*CNR-SPIN and Dipartimento di Fisica, "E. R. Caianiello," Via Ponte don Mellillo, I-84084 Fisciano Salerno, Italy*

[4]*Berliner Elektronenspeicherring-Gesellschaft für Synchrotronstrahlung m.b.H., Albert-Einstein Strasse 15, D-12489 Berlin, Germany*

(Received 25 April 2012; published 14 June 2012)

The optical conductivity $\sigma(\omega)$ of $Sr_4Ru_3O_{10}$ has been studied by means of reflectivity measurements between 12 and 300 K both in the ab planes (from 40 to 28 000 cm^{-1}) and along the c axis (from 40 to 19 000 cm^{-1}). In the far and mid infrared, $\sigma_{ab}(\omega)$ results from a superposition of a Drude term, with a plasma frequency which increases below the ferromagnetic transition at $T_c = 105$ K, and of two bands in the infrared. One is peaked at about 400 cm^{-1} for $T < 300$ K, but softens to 300 cm^{-1} at room temperature. The other one is peaked at 1300 cm^{-1} and, below T_c, provides spectral weight to the Drude term, suggesting that it has a magnetic origin. Along the c axis, $\sigma_c(\omega)$ is instead that of a good insulator, with phonon peaks whose frequencies ω_{ph} regularly increase as T decreases. For the mode at the highest frequency, however, which can be assigned to the apical oxygens of the RuO_6 octahedra, both ω_{ph} and the intensity I_{ph} have an anomalous behavior below T_c.

DOI: 10.1103/PhysRevB.85.235124 PACS number(s): 74.70.Pq, 78.30.−j, 78.20.−e

I. INTRODUCTION

The perovskites belonging to the Ruddlesden-Popper (RP)-type series $Sr_{n+1}Ru_nO_{3n+1}$ ($n = 1$, 2, 3, and ∞) present peculiar and interesting phenomena, like the unconventional superconductivity of Sr_2RuO_4 ($n = 1$), where the Cooper pairs are in a p-symmetry triplet state,[1] the metamagnetism[2] and quantum criticality exhibited by $Sr_3Ru_2O_7$ ($n = 2$) at $T \lesssim 1$ K,[3,4] and the unusual ferromagnetism of $SrRuO_3$ ($n = \infty$).[5] The optical properties of the RP series have been studied in Refs. 6 and 7 (Sr_2RuO_4), in Ref. 8 ($SrRuO_3$), and in Refs. 9–11 ($Sr_3Ru_2O_7$). The latter compound exhibits a strong anisotropy in the optical conductivity. The ab plane is metallic, but shows a crossover around 300 K to a high-T regime characterized by a strongly enhanced scattering rate. Along the c axis, the Drude term has a much smaller plasma frequency, and a strong absorption appears at 1 eV. These findings indicate an anisotropic metallic state where electron-electron and electron-phonon interactions play a major role.[11] The compound with $n = 3$, $Sr_4Ru_3O_{10}$, is the less-studied member of the series. Its orthorhombic unit cell is composed of triple layers of corner-shared RuO_6 octahedra separated by double rock-salt layers of Sr-O. Within each triple layer, the octahedra in both outer layers are rotated by 5.6°, while those in the central layer are rotated by 11° in the opposite direction.[12] Accurate transport and magnetic measurements on flux-grown crystals[12] showed that $Sr_4Ru_3O_{10}$ becomes ferromagnetic below a Curie temperature $T_C = 105$ K. This occurs under low magnetic fields if $\vec{B}$ is directed along the c axis while, if $\vec{B}$ is in the ab plane, a metamagnetic transition[13] is observed at $T_M = 50$ K. It has been suggested recently[14] that the latter transition, which is accompanied by anomalies in the specific heat,[15] in the thermopower,[16] and in the spin-phonon interaction,[17] originates from the $d_{xz,yz}$ Ru orbitals.

Moreover, from x-ray-absorption spectroscopy measurements it has been inferred[18] that metamagnetism in $Sr_4Ru_3O_{10}$ and $Sr_3Ru_2O_7$ may be related to a rearrangement of the t_{2g} orbital occupation as n increases. This effect is controlled by an interplay of Coulomb repulsion, dimensionality, and changes in the t_{2g} crystal field.

The ab plane resistivity, $\rho_{ab}(T)$, of $Sr_4Ru_3O_{10}$ crystals turned out to be that of a good metal and was found to increase quasilinearly from about 20 to 300 K, with changes of slope at T_c and T_M.[19] At lower T, however, the T dependence of ρ_{ab} is quadratic, indicating that the ground state of the electrons is a Fermi liquid. The resistivity along the c axis, $\rho_c(T)$, was found to be that of a poor metal, as it increased with T but was larger than ρ_{ab} by about three orders of magnitude at any T.[19] Other authors[13] reported a rapid drop in $\rho_c(T)$ when cooling the sample below T_M. A strong anisotropy is also present both in the magnetic susceptibility, with $\chi_c/\chi_{ab} = 29$ in the region where the Curie-Weiss law holds (i.e., from 150 to 350 K),[13] and in the magnetoresistance.[14] In the present paper we report those which, to our knowledge, are the first infrared spectra of $Sr_4Ru_3O_{10}$. In order to observe how its anisotropic transport and magnetic properties reflect on its optical response, we have performed reflectivity measurements on a single crystal grown by the floating zone (FZ) technique, with the radiation polarized both in the ab plane and along the c axis. The present data extend to $Sr_4Ru_3O_{10}$ an optical study of the RP-type series that we began with[11] $Sr_3Ru_2O_7$.

II. EXPERIMENT AND RESULTS

A. Samples and procedure

Single crystals of $Sr_4Ru_3O_{10}$ were grown by the flux-feeding floating-zone method with Ru self-flux in a commercial image furnace. The ceramic feed rods were prepared by a standard solid-state reaction method, from $SrCO_3$ (99.99% purity) and RuO_2 (99.9%). The powders were mixed with an appropriate molar ratio of Sr/Ru, fired and sintered in air at 1450 °C for 18 h and at 1420 °C for 2 h, respectively. For the crystal growth we used a 6-mm-diameter feed rod and $Sr_4Ru_3O_{10}$ crystals from previous growth as seed. Growth speed, atmosphere, and pressure were selected on the basis of previous experience,[20] to obtain pure $Sr_4Ru_3O_{10}$ single

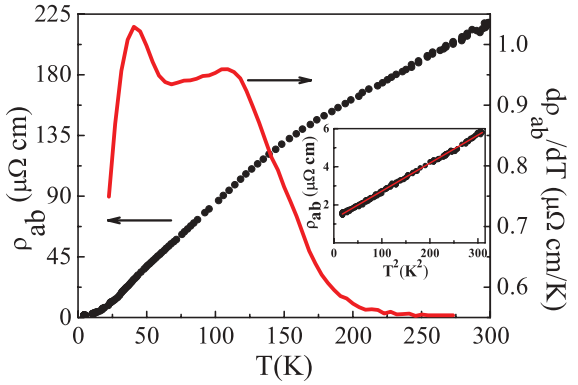

FIG. 1. (Color online) Resistivity vs temperature of a $Sr_4Ru_3O_{10}$ single crystal from the same batch as that used for the optical measurements, measured with the electrodes in the *ab* plane (black line, left scale) and its derivative with respect to temperature (red line, right scale). The inset shows $\rho_{ab}(T)$ on a T^2 scale in the temperature range 4.2–18 K (dots) and the fit (red line) to Eq. (1).

crystals. They tend to cleave parallel to the growth direction as in the other members of the series. As shown by high-resolution x-ray diffraction, the cleaved surface is the *ab* plane. The *c*-axis lattice constant was 2.8577(11) nm. The crystal surface was investigated by polarized light optical microscopy (PLOM) and by scanning electron microscopy (SEM). The compositional analysis was carried out by energy dispersive spectroscopy (EDS), while the crystal microstructure and the local orientation were studied by means of electron back-scattered diffraction (EBSD). We measured the transport properties of the $Sr_4Ru_3O_{10}$ crystals by a standard lock-in technique at 91.285 Hz with a current of 0.5 mA in the *ab* plane, and finally adjusted by taking into account the $\rho(T)$ values in Fig. 1.

The quality of the $Sr_4Ru_3O_{10}$ crystals was finally controlled by measuring the resistivity $\rho_{ab}(T)$ at low temperature, with a 0.5-mA current parallel to the *ab* plane. The electrical connections were made of gold wire and high-temperature cured (500 °C for 5 min) silver epoxy (Dupont 6838). The crystal was extracted from the same batch as that employed for the optical measurements, and its dimensions were about $2 \times 0.5 \times 0.2\ \text{mm}^3$. The resulting resistivity is shown in Fig. 1 from 4.2 to 300 K. Two slight changes of slope are observed: one around T_c, where also the free-carrier plasma frequency changes (see below), and another one, around 50 K, which may be related to the metamagnetic transition.[13,14,17] Both of them are more clearly shown by the derivative $d\rho_{ab}/dT$, which is plotted in the same figure vs the right scale. The inset shows instead the quadratic temperature dependence of $\rho_{ab}(T)$ at low temperature. Indeed, in the range 4.2–18 K the data could be fit (red line) by

$$\rho_{ab} = \rho_0 + AT^2 \tag{1}$$

with $\rho_0 = 1.25\ \mu\Omega\,\text{cm}$ and $A = 1.47 \times 10^{-2}\ \mu\Omega\,\text{cm/K}^2$. These values confirm the high quality of the crystals. Indeed, the value $\rho_0 < 2\ \mu\Omega\,\text{cm}$ is comparable to that found in the best other members of the same RP family.[1,21] Moreover, the excellent agreement between data and Eq. (1) confirms that the electronic ground state of $Sr_4Ru_3O_{10}$ is a Fermi liquid.[19]

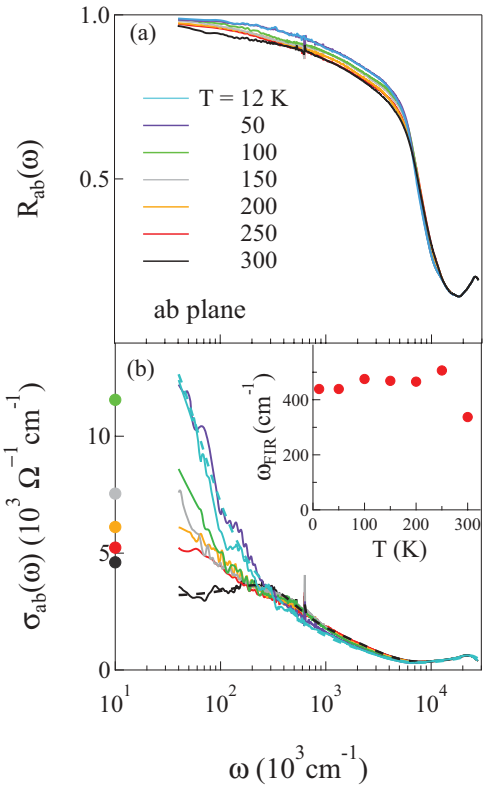

FIG. 2. (Color online) Reflectivity (a) and optical conductivity (b) of the *ab* plane of $Sr_4Ru_3O_{10}$ between 12 and 300 K. The dots on the vertical axis in (b) are the dc-conductivity values extracted at the corresponding temperatures from Fig. 1. Those at the lowest temperatures are out of scale. The dashed lines are examples of the fits to a Drude-Lorentz model. They provide the parameters plotted in Fig. 3 and here in the inset, where the peak frequency of the FIR contribution to $\sigma_{ab}(\omega)$ is reported vs temperature.

The sample used for the optical experiment came from the same batch as that used for the above quasi-dc measurements and its dimensions were about $4.3 \times 2 \times 1.6\ \text{mm}^3$. The reflectivity $R(\omega)$ of the crystal was measured with the radiation polarized either along the *c* axis (1.6 mm long) or in the *ab* plane, at nearly normal incidence (8°). The reference was obtained by evaporating *in situ* onto the sample a gold film for the far and mid infrared, and a silver film for the near infrared and the visible range. Data were collected by a rapid-scanning interferometer from 40 to 28 000 cm^{-1} in the *ab* planes and from 40 to 19 000 cm^{-1} along the *c* axis. The samples were thermoregulated within ±2 K at various temperatures between 12 and 300 K. The real part of the optical conductivity $\sigma(\omega)$ was extracted from the reflectivity by Kramers-Kronig transformations and standard extrapolations to infinite frequency. The extrapolation to zero frequency was obtained by Drude-Lorentz fits to the measured far-infrared reflectivity.

B. Optical properties of the *ab* plane

The *ab* plane reflectivity $R_{ab}(\omega)$ of $Sr_4Ru_3O_{10}$, as measured from 12 to 300 K and from 40 to 28 000 cm^{-1}, is shown in Fig. 2(a). As T is lowered, $R_{ab}(\omega)$ increases monotonically in the far and mid infrared, and decreases slightly in the near

infrared. The isosbestic point is situated around 10 000 cm^{-1}. The plasma edge at ~15 000 cm^{-1} indicates that the system is a good metal.

The optical conductivity $\sigma_{ab}(\omega)$ extracted from $R_{ab}(\omega)$ through the Kramers-Kronig transformations is shown in Fig. 2(b). It is basically Drude like at all temperatures, with a pronounced increase of the Drude absorption below 100 K, and a clear decrease at 300 K. At this temperature a broad peak becomes evident in the far-infrared (FIR) band, at $\omega_{FIR} \sim 300$ cm^{-1}. The far-infrared behavior of $\sigma_{ab}(\omega)$ at 300 K is suggestive of partially incoherent hopping, as observed in some cuprates at high temperature.[22]

C. Drude-Lorentz analysis of $\sigma_{ab}(\omega)$

In order to get further insight on the competition between transport and localization in $Sr_4Ru_3O_{10}$, we analyzed the optical response of the ab plane by fitting $\sigma_{ab}(\omega)$ to the usual Drude-Lorentz dielectric function,

$$\begin{aligned}\tilde{\epsilon}(\omega) &= \epsilon_1(\omega) + i\epsilon_2(\omega) \\ &= \epsilon_\infty - \frac{\omega_p^2}{\omega^2 - i\omega\Gamma} + \frac{S_{FIR}^2}{\left(\omega_{FIR}^2 - \omega^2\right) - i\omega\Gamma_{FIR}} \\ &\quad + \frac{S_{MIR}^2}{\left(\omega_{MIR}^2 - \omega^2\right) - i\omega\Gamma_{MIR}} + \frac{S_{el}^2}{\left(\omega_{el}^2 - \omega^2\right) - i\omega\Gamma_{el}},\end{aligned} \tag{2}$$

where $\epsilon_2(\omega) = (4\pi/\omega)\sigma_{ab}(\omega)$. In the right-hand side of Eq. (2), ϵ_∞ replaces all contributions at energies higher than the measuring range, while the second term is the Drude contribution with plasma frequency ω_p and relaxation rate Γ. As all phonon modes are well screened by the free carriers, one has here to add to the Drude absorption a FIR band with strength S_{FIR} and width Γ_{FIR}, a MIR band with strength S_{MIR} and width Γ_{MIR}, and a broad interband contribution peaked at $\omega_{el} = 22\,000$ cm^{-1}. Two examples of the fits are shown by the dashed lines in Fig. 2(b).

The parameters of the FIR band and of the Drude absorption are reported vs temperature in the inset of Figs. 2(b) and in 3, together with the intensity of the MIR band (its peak frequency of 1300 cm^{-1} does not change appreciably with temperature). Therein one sees that the FIR band is present at all temperatures, at frequencies higher than at 300 K. In Fig. 3(a) the intensity of the Drude term ω_p^2 has an interesting behavior. On one hand, at 300 K it decreases by transferring spectral weight to the FIR band (which also softens as remarked above). This implies that a fraction of localized charges exists at all temperatures in $Sr_4Ru_3O_{10}$, and that it increases at high temperature probably due to disorder (as in[11] $Sr_3Ru_2O_7$). On the other hand, ω_p increases below the ferromagnetic transition at T_c, probably through a transfer of spectral weight to the Drude term from the MIR band (as we have proposed by means of the dashed lines in Fig. 3). This partial delocalization of the MIR band below T_c suggests that it may be attributed to a magnetic polaron, as has been proposed for the corresponding band of the cuprates.[23] Finally, the carrier relaxation rate Γ in Fig. 3(b) increases linearly with temperature over the whole measuring range, consistently with the quasilinear increase in the resistivity reported in Fig. 1.

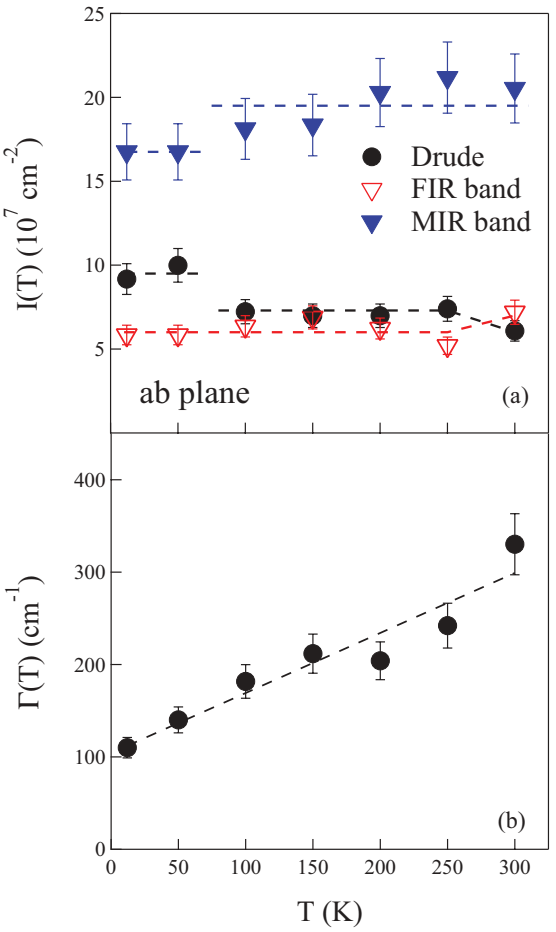

FIG. 3. (Color online) Parameters vs. temperature of the Drude-Lorentz fits to the ab-plane optical conductivity of $Sr_4Ru_3O_{10}$: (a) intensities of the Drude component (ω_p^2), of the FIR band (S_{FIR}^2), and of the midinfrared (MIR) band (S_{MIR}^2); (b) free-carrier relaxation rate, or Drude linewidth, Γ.

D. Extended-Drude analysis of $\sigma_{ab}(\omega)$

An alternative analysis of $\sigma_{ab}(\omega)$ is based on the extended-Drude model.[24] In this case, the complex dielectric function is written in terms of a frequency-dependent, optical relaxation rate

$$\Gamma(\omega) = -\frac{\omega_p^2}{\omega}\mathrm{Im}\left(\frac{1}{\tilde{\epsilon}(\omega) - \epsilon_\infty}\right) \tag{3}$$

and of a frequency-dependent effective mass

$$\frac{m^*(\omega)}{m_b} = -\frac{\omega_p^2}{\omega^2}\mathrm{Re}\left(\frac{1}{\tilde{\epsilon}(\omega) - \epsilon_\infty}\right). \tag{4}$$

Here m_b is the band mass, which is not known and therefore assumed, as usual, to be the free-electron mass, while $\epsilon_\infty = 1.2$ is the contribution from the high-frequency interband transitions. The determination of ω_p in Eqs. (3) and (4) is a crucial issue. In the present case, its choice is facilitated by the presence of a sharp edge in the reflectivity around 15 000 cm^{-1}, which separates the intraband from the interband contributions. By subtracting from the former term the low-frequency tail of the interband transitions, which is reconstructed through a

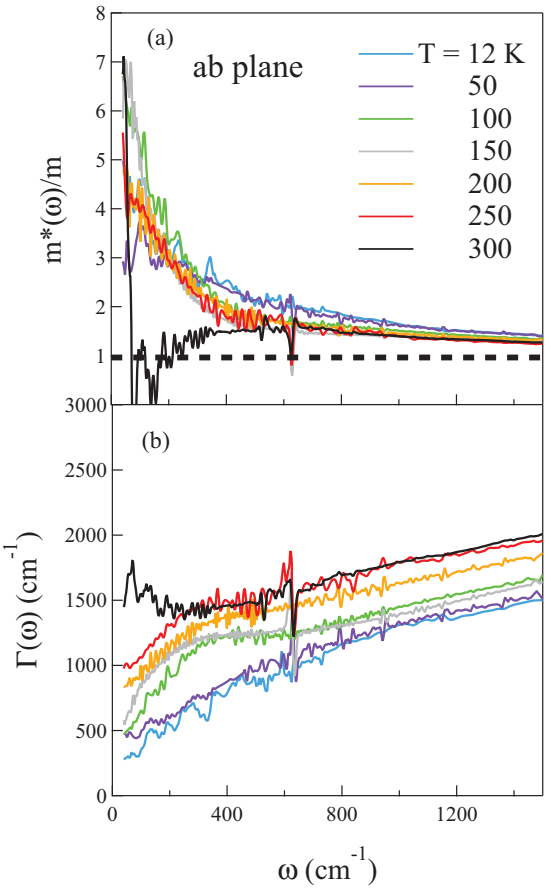

FIG. 4. (Color online) Frequency-dependent effective mass (a) and relaxation rate (b) as extracted by Eqs. (3) and (4) from the $\sigma_{ab}(\omega)$ of Fig. 2(b).

Lorentzian fit, ω_p was corrected to 18 000 cm^{-1}. The results are reported in Fig. 4. As expected, they are unreliable at 300 K, where the appearance of a pronounced FIR band prevents any reasonable application of a single-component model. Nevertheless, $m^*(\omega)$ in Fig. 4(a) approaches the band mass m_b at high energy at any temperature, as it should, while at low frequency and temperature $m^* \sim 6m_b$. This enhancement of the effective mass in the far infrared is consistent with recent results on different pnictides.[25,26] In turn, the low-frequency behavior of $\Gamma(\omega)$ in Fig. 4(b) excludes the presence of a pseudogap[24] in the whole temperature range where the present model provides reliable results. One may notice that $\Gamma(\omega)$ exceeds the value of ω in the far infrared, as already reported for some cuprates.[24,27] Therefore the basic assumption of the Fermi-liquid theory $1/\tau(\omega) < \omega/2\pi$, which is required for the coherence of quasiparticles, is fulfilled only above a frequency ω_0 which at high T falls in the mid infrared. However, it decreases strongly at the lowest temperatures, where ω_0 is smaller than ω_p by a factor of 40. This may explain the Fermi-liquid behavior of $\rho(T)$ in the inset of Fig. 1 below 18 K.

E. Spectral weight in the *ab* plane

The *ab*-plane optical conductivity of $Sr_4Ru_3O_{10}$ can be integrated to obtain the spectral weight $W(\Omega,T)$, a model-independent quantity defined as

$$W(\Omega,T) = \frac{2m^*V}{\pi e^2}\int_0^{\Omega}\sigma_{ab}(\omega,T)d\omega. \qquad (5)$$

Here m^* is the effective mass of the carriers (assumed again to be the free-electron mass) and V is the volume of the formula-unit cell. The resulting W is plotted in Fig. 5 vs the cutoff frequency Ω at different temperatures. According to the f-sum rule on W, all those curves should collapse into a single one for $\Omega \to \infty$. As shown in the figure, this happens for $\Omega \sim \Omega_p$, where Ω_p is the reflectivity plasma edge, namely the plasma frequency renormalized by the screening effect of the higher-energy bound charges. Such a "restricted sum rule" is verified in many metals, not in strongly correlated oxides like the high-T_c superconductors[28] or V_2O_3,[29] neither in a rutenate like[11] $Sr_3Ru_2O_7$.

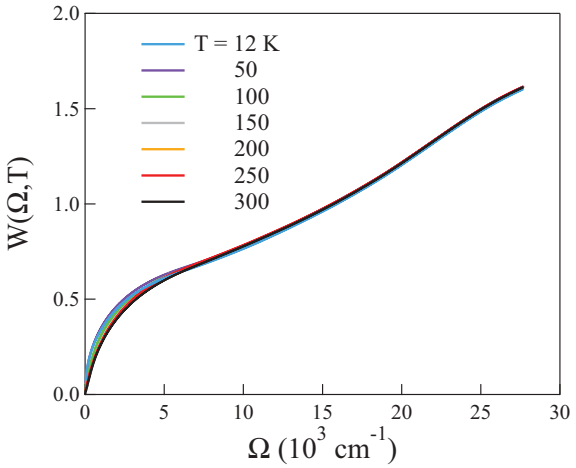

FIG. 5. (Color online) Spectral weight of $Sr_4Ru_3O_{10}$ in the *ab* plane vs the cutoff frequency in Eq. (5), at selected temperatures between 12 and 300 K.

In general, the spectral weight depends on temperature as[28]

$$W(\Omega,T) = W_0[1 - b(\Omega)T^2]. \qquad (6)$$

The above quadratic dependence is expected on the basis of a one-band tight-binding model and of a Sommerfeld expansion of the kinetic energy. In a conventional metal like gold, both W_0 and b are controlled by the same energy scale, namely the hopping rate t. In some oxides instead, the former scale is much larger than that which controls the frequency-dependent coefficient b, which describes the "thermal response" of the carriers. On the basis of dynamical mean-field theory (DMFT) calculations, it was shown that this peculiar behavior is related to their strong correlation effects.[30] As here we obtained a good agreement with Eq. (6) at any Ω, we could extract from the fits $b(\Omega)$. This quantity is plotted in Fig. 6 for $Sr_4Ru_3O_{10}$, and compared therein with that of $Sr_3Ru_2O_7$, of the superconducting cuprate $La_{1.88}Sr_{0.12}CuO_4$, and of a conventional metal like gold. In order to facilitate the comparison, $b(\Omega)$ is reported vs Ω/Ω_p, where Ω_p is the plasma edge of each compound: 18 000, 9000, 6500, and 20 500 cm^{-1}, respectively. In correlated materials, unlike in a conventional Fermi liquid, $b(\Omega)$ is appreciably different from zero well beyond the plasma edge,[28–30] while in a

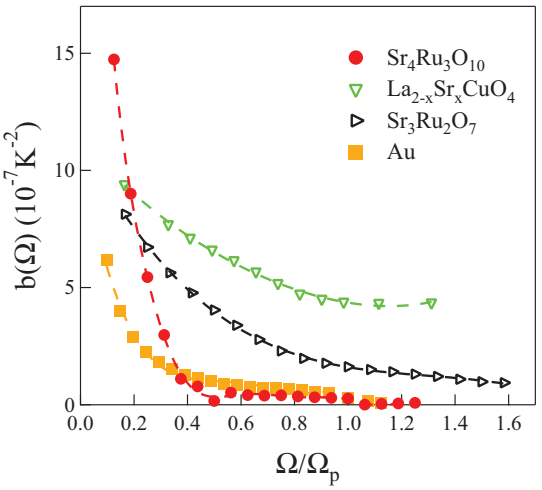

FIG. 6. (Color online) Thermal coefficient $b(\Omega)$ in the ab plane of $Sr_4Ru_3O_{10}$ vs a normalized cutoff frequency, extracted from Eq. (6) and compared with the $b(\Omega)$ of other oxides like $Sr_3Ru_2O_7$ and $La_{1.88}Sr_{0.12}CuO_4$, and with that of a conventional metal like gold. Dashed lines are just guides to the eye.

conventional metal like gold $b(\Omega) \simeq 0$ at Ω_p. Figure 6 shows that in $Sr_4Ru_3O_{10}$, as already mentioned, the restricted sum rule works nearly as well as in gold. In $Sr_3Ru_2O_7$ instead, the behavior of $b(\Omega)$ is intermediate between that of gold and that of the superconducting cuprate. Therefore from the present analysis one may conclude that in $Sr_4Ru_3O_{10}$ the effect of electron correlations is much weaker than in the same-family member $Sr_3Ru_2O_7$ and in a cuprate like $La_{2-x}Sr_xCuO_4$.

F. Optical conductivity of the *c* axis

The reflectivity $R_c(\omega)$ of $Sr_4Ru_3O_{10}$, as measured with the radiation field polarized along the c axis of its crystal structure, is shown in Fig. 7(a) from 12 to 300 K. The optical conductivity $\sigma_c(\omega)$, extracted from those data through the Kramers-Kronig transformations, is reported in Fig. 7(b) and looks like that of a good insulator. For $\omega \to 0$, at low T $\sigma_c \approx 100\ \Omega^{-1}\,cm^{-1}$, while in $Sr_3Ru_2O_7$, along the c axis, we found about $700\ \Omega^{-1}\,cm^{-1}$.[11] The dc measurements provide instead, in both compounds, $\rho_c \sim 2\ m\Omega\,cm$ at 10 K.[13,19,31] The large discrepancy for $Sr_4Ru_3O_{10}$ may be attributed to the large error which affects the infrared determination when the conductivity is so low as in Fig. 7(b).

In Fig. 7(b) four phonon peaks are clearly distinguished, together with a broad absorption in the near-infrared peaked at $\sim 5000\ cm^{-1}$, which can be assigned to an electronic interband transition and determines the optical gap at $\sim 2000\ cm^{-1}$ or 0.25 eV. Five Raman modes were instead detected in the zz polarization.[32] A further comparison can be made with the c axis of $Sr_3Ru_2O_7$, where three phonon modes, partially shielded by the free carriers, were observed at 306, 382, and $440\ cm^{-1}$. The behavior with temperature of the infrared peak frequencies ω_{ph} is shown in Fig. 8. Modes 1, 2, and 3 exhibit the usual hardening for decreasing temperature, due to the crystal contraction. The highest-frequency mode 4, which can be attributed to the vibration, along the c axis, of the apical oxygens of the RuO_6 octahedra,[32] is instead anomalous, in

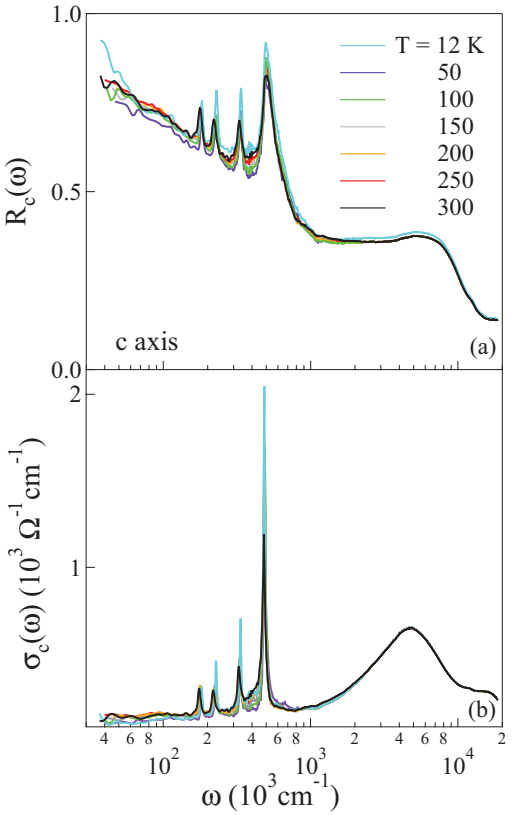

FIG. 7. (Color online) Reflectivity (a) and optical conductivity (b) of $Sr_4Ru_3O_{10}$, as measured between 12 and 300 K, with the radiation field parallel to the the c axis.

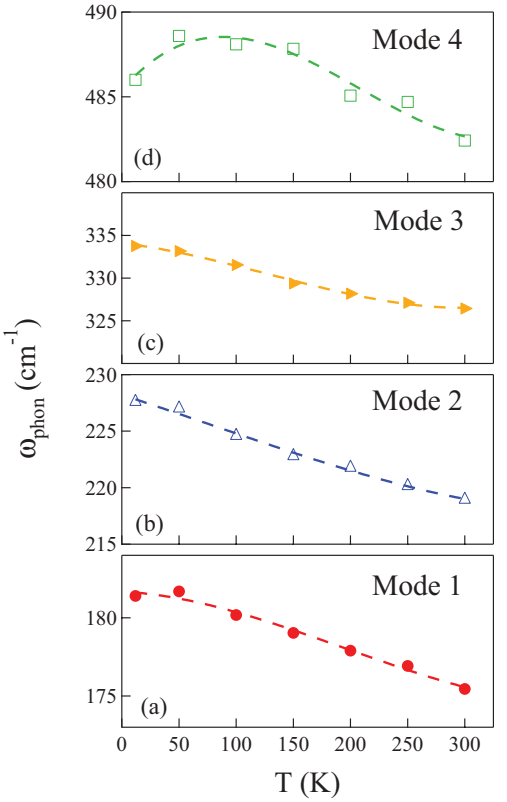

FIG. 8. (Color online) Peak frequency versus temperature of the infrared active phonons observed along the c axis in $Sr_4Ru_3O_{10}$.

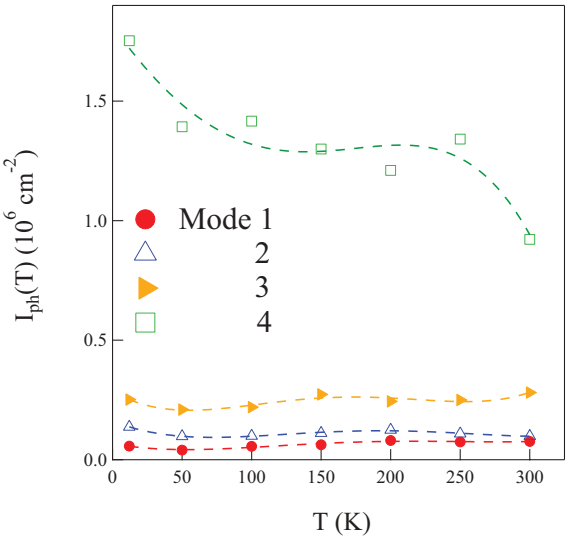

FIG. 9. (Color online) Intensity versus temperature of the infrared-active phonon modes along the c axis of $Sr_4Ru_3O_{10}$.

that its frequency ω_{ph} starts from 482 cm^{-1} at 300 K, reaches a maximum at 489 cm^{-1} between 100 and 50 K, namely between T_c and T_M, and decreases again to 486 cm^{-1} at 12 K. Also its intensity I_{ph} is strongly sensitive to temperature below 100 K, as shown in Fig. 9. The apical-oxygen phonon anomaly might be related to the 0.2% elongation of the crystal c axis that was observed when cooling the crystal to 90 K.[13] However, anomalies were observed also in the phonon Raman spectra of the ab plane at approximately the same temperatures,[32] and similar features were found as a function of magnetic field and pressure.[17] Therefore the anomalous behavior of the optical phonons points out a coupling between the lattice and the magnetic degrees of freedom of the ruthenate, most likely through the orbital degrees of freedom.[13]

III. CONCLUSION

The present paper follows a previous infrared study of the member with $n = 2$ of the RP-type series, $Sr_3Ru_2O_7$. Here we have studied the optical conductivity of $Sr_4Ru_3O_{10}$, the member with $n = 3$, with the radiation field polarized both in the ab plane and along the c axis. Its $\sigma_{ab}(\omega)$ is similar to that of a good metal, with a plasma edge falling at the beginning of the visible range around 15 000 cm^{-1}. This is confirmed by the temperature dependence of the thermal coefficient $b(\Omega)$ of the spectral weight, which is closer to that of a conventional metal like gold than to those of oxides with strong correlation. The carrier relaxation rate Γ increases linearly vs temperature and, at low temperature, the resistivity increases with T^2 as expected for a Fermi liquid.

Nevertheless, when analyzed in further detail, the free-carrier absorption of $Sr_4Ru_3O_{10}$ exhibits some peculiar features. The plasma frequency decreases appreciably at 300 K, by transferring spectral weight to a far-infrared oscillator that survives down to the lowest temperatures. As in many other oxides, the FIR band is suggestive of localized charges, either self-trapped by the electron-phonon interaction (polarons), or bound to impurities. As in most cuprates, a second oscillator is observed, the midinfrared band at about 1300 cm^{-1}. This may be tentatively assigned to a magnetic polaron, as it appears to lose intensity and transfer spectral weight to the Drude term below the magnetic ordering temperature T_c. The extended-Drude analysis does not detect the presence of a pseudogap in the density of states but shows that $\Gamma(\omega) > \omega$ up to midinfrared frequencies. At low temperature, however, this violation of the basic requirement for a Fermi-liquid behavior affects only a small fraction of the electron frequencies (with respect to the plasma frequency). This may explain why $\rho(T) \propto T^2$ below 18 K in Fig. 1.

The measurements along the c axis point out the very strong anisotropy of this crystal, which is a better metal than $Sr_3Ru_2O_7$ in the basal plane, and a comparable insulator along the c axis. In its optical conductivity, four well defined phonon peaks in the far infrared and an interband transition around 5000 cm^{-1} are observed. The highest-frequency phonon, which can be assigned to the vibration of the apical oxygens of the RuO_6 octahedra, shows an anomaly in its peak frequency below 100 K, which can be compared to those reported in the literature for the Raman modes of the ab plane, and which confirms the coupling between the lattice and the spin states of the system, most likely through the orbital degrees of freedom.

ACKNOWLEDGMENTS

The authors acknowledge useful discussions with C. Attanasio, C. Cirillo, and G. Patimo. U. Gambardella and A. Ferrentino kindly provided liquid helium. We acknowledge the Helmholtz-Zentrum Berlin electron storage ring BESSY II for provision of synchrotron radiation at beamline IRIS. The research leading to these results has received funding from the European Community's Seventh Framework Programme (FP7/2007-2013) under Grant No. n.226716. R.F. also acknowledges support from the FP7/2007-2013 program under Grant No. 264098-MAMA.

[1] A. P. Mackenzie and Y. Maeno, Rev. Mod. Phys. **75**, 657 (2003), and references therein.

[2] R. S. Perry, L. M. Galvin, S. A. Grigera, L. Capogna, A. J. Schofield, A. P. Mackenzie, M. Chiao, S. R. Julian, S. I. Ikeda, S. Nakatsuji, Y. Maeno, and C. Pfleiderer, Phys. Rev. Lett. **86**, 2661 (2001).

[3] A. G. Green, S. A. Grigera, R. A. Borzi, A. P. Mackenzie, R. S. Perry, and B. D. Simons, Phys. Rev. Lett. **95**, 086402 (2005), and references therein.

[4] A. Tamai, M. P. Allan, J. F. Mercure, W. Meevasana, R. Dunkel, D. H. Lu, R. S. Perry, A. P. Mackenzie, D. J. Singh, Z.-X. Shen, and F. Baumberger, Phys. Rev. Lett. **101**, 026407 (2008).

[5] L. Klein, J. S. Dodge, C. H. Ahn, G. J. Snyder, T. H. Geballe, M. R. Beasley, and A. Kapitulnik, Phys. Rev. Lett. **77**, 2774 (1996).

[6] T. Katsufuji, M. Kasai, and Y. Tokura, Phys. Rev. Lett. **76**, 126 (1996).

[7]M. G. Hildebrand, M. Reedyk, T. Katsufuji, and Y. Tokura, Phys. Rev. Lett. **87**, 227002 (2001).
[8]P. Kostic, Y. Okada, N. C. Collins, Z. Schlesinger, J. W. Reiner, L. Klein, A. Kapitulnik, T. H. Geballe, and M. R. Beasley, Phys. Rev. Lett. **81**, 2498 (1998).
[9]A. V. Puchkov, M. C. Schabel, D. N. Basov, T. Startseva, G. Cao, T. Timusk, and Z.-X. Shen, Phys. Rev. Lett. **81**, 2747 (1998).
[10]J. S. Lee, Y. S. Lee, T. W. Noh, S. Nakatsuji, H. Fukazawa, R. S. Perry, Y. Maeno, Y. Yoshida, S. I. Ikeda, J. Yu, and C. B. Eom, Phys. Rev. B **70**, 085103 (2004).
[11]C. Mirri, L. Baldassarre, S. Lupi, M. Ortolani, R. Fittipaldi, A. Vecchione, and P. Calvani, Phys. Rev. B **78**, 155132 (2008).
[12]M. K. Crawford, R. L. Harlow, W. Marshall, Z. Li, G. Cao, R. L. Lindstrom, Q. Huang, and J. W. Lynn, Phys. Rev. B **65**, 214412 (2002).
[13]G. Cao, L. Balicas, W. H. Song, Y. P. Sun, Y. Xin, V. A. Bondarenko, J. W. Brill, S. Parkin, and X. N. Lin, Phys. Rev. B **68**, 174409 (2003).
[14]D. Fobes, T. J. Liu, Z. Qu, M. Zhou, J. Hooper, M. Salamon, and Z. Q. Mao, Phys. Rev. B **81**, 172402 (2010).
[15]G. Cao, S. Chikara, J. W. Brill, and P. Schlottmann, Phys. Rev. B **75**, 024429 (2007).
[16]Z. Xu, X. Xu, R. S. Freitas, Z. Long, M. Zhou, D. Fobes, M. Fang, P. Schiffer, Z. Mao, and Y. Liu, Phys. Rev. B **76**, 094405 (2007).
[17]R. Gupta, M. Kim, H. Barath, S. L. Cooper, and G. Cao, Phys. Rev. Lett. **96**, 067004 (2006).
[18]M. Malvestuto, E. Carleschi, R. Fittipaldi, E. Gorelov, E. Pavarini, M. Cuoco, Y. Maeno, F. Parmigiani, and A. Vecchione, Phys. Rev. B **83**, 165121 (2011).
[19]M. Zhou, J. Hooper, D. Fobes, Z. Q. Mao, V. Golub, and C. J. O'Connor, Mat. Res. Bull. **40**, 942 (2005).
[20]R. Fittipaldi, V. Granata, and A. Vecchione, Cryst. Res. Technol. **46**, 769 (2011).
[21]R. S. Perry, K. Kitagawa, S. A. Grigera, R. A. Borzi, A. P. Mackenzie, K. Ishida, and Y. Maeno, Phys. Rev. Lett. **92**, 166602 (2004).
[22]D. Nicoletti, P. Di Pietro, O. Limaj, P. Calvani, S. Ono, Y. Ando, and S. Lupi, New J. Phys. **13**, 123009 (2011).
[23]A. S. Mishchenko, N. Nagaosa, Z. X. Shen, G. De Filippis, V. Cataudella, T. P. Devereaux, C. Bernhard, K. W. Kim, and J. Zaanen, Phys. Rev. Lett. **100**, 166401 (2008).
[24]For a review, see T. Timusk and B. Statt, Rep. Prog. Phys. **62**, 61 (1999).
[25]D. Wu, N. Barisic, N. Drichko, S. Kaiser, A. Faridian, M. Dressel, S. Jiang, Z. Ren, L. J. Li, G. H. Cao, Z. A. Xu, H. S. Jeevan, and P. Gegenwart, Phys. Rev. B **79**, 155103 (2009).
[26]M. M. Qazilbash, J. J. Hamlin, R. E. Baumbach, L. Zhang, D. J. Singh, M. B. Maple, and D. N. Basov, Nat. Phys. **5**, 647 (2009).
[27]D. N. Basov and T. Timusk, Rev. Mod. Phys. **77**, 721 (2005).
[28]M. Ortolani, P. Calvani, and S. Lupi, Phys. Rev. Lett. **94**, 067002 (2005).
[29]L. Baldassarre, A. Perucchi, D. Nicoletti, A. Toschi, G. Sangiovanni, K. Held, M. Capone, M. Ortolani, L. Malavasi, M. Marsi, P. Metcalf, P. Postorino, and S. Lupi, Phys. Rev. B **77**, 113107 (2008).
[30]A. Toschi, M. Capone, M. Ortolani, P. Calvani, S. Lupi, and C. Castellani, Phys. Rev. Lett. **95**, 097002 (2005).
[31]S.-I. Ikeda, Y. Maeno, S. Nakatsuji, M. Kosaka, and Y. Uwatoko, Phys. Rev. B **62**, R6089 (2000).
[32]M. N. Iliev, V. N. Popov, A. P. Litvinchuk, M. V. Abrashev, J. Bäckström, Y. Y. Sun, R. L. Meng, and C. W. Chu, Physica B **358**, 138 (2005).